Polymer Chemistry

Accepted Manuscript

ROYAL SOCIETY OF CHEMISTRY

www.rsc.org/polymers

Cite this: DOI: 10.1039/c0xx00000x

www.rsc.org/xxxxxx

ARTICLE TYPE

Synthetic glycopolypeptides: Synthesis and self-assembly of poly(γ-benzyl-L-glutamate)-glycosylated dendron hybrids

Ariane Peyret,[a] John F. Trant,[b] Colin V. Bonduelle,[a,c] Khalid Ferji,[a] Namrata Jain,[b] Sebastien Lecommandoux,[a]* and Elizabeth R. Gillies[b,d]*

Received (in XXX, XXX) Xth XXXXXXXXX 20XX, Accepted Xth XXXXXXXXX 20XX
DOI: 10.1039/b000000x

Nano-assemblies prepared from glycosylated macromolecules are promising systems for modulating or mimicking the interactions between natural carbohydrates and their receptors. In the current work, polyester dendrons bearing focal point alkynes and peripheral *C*-linked α-galactose moieties were synthesized and coupled to helical poly(γ-benzyl-*L*-glutamate) (PBLG) to afford synthetic linear-dendritic glycopolypeptides. Both the dendrimer generation and the length of the PBLG were varied to provide a small library of amphiphiles with hydrophilic mass fractions ranging from 0.07 to 0.54. The self-assembly of the copolymers in water using a solvent exchange method was optimized and studied in detail. While the linear-dendritic copolymers composed of lower generation dendrons tended to aggregate, a copolymer composed of a 4th generation galactose-functionalized dendron and PBLG with a degree of polymerization of 28 formed micellar nano-assemblies whose size could be tuned by varying the self-assembly process. Overall, this study provides new insights into the effects of polymer architecture on self-assembly properties, while at the same time introducing a new platform for the preparation of bioactive nanoparticles.

Introduction

Block copolymers are complex macromolecules that allow the properties of individual polymer segments to be introduced within single molecules, while also allowing for the generation of new properties through synergistic combinations of different blocks.[1,2] As a representative example, macromolecular self-assembly can be induced in either the bulk or solution phase due to the thermodynamic incompatibility and/or solvent selectivity of the different blocks. The nanomaterials that result from the self-assembly of amphiphilic macromolecules in a selective solvent offer a wide scope of possibilities and open doors to many different applications in nanoscience and nanotechnology.[3] Important factors that determine the morphology obtained from these macromolecular structures are the volume ratio of the hydrophilic and hydrophobic blocks as well as the processing conditions.[4] Assemblies of amphiphilic macromolecules have generated increasing interest over the past few decades for applications such as drug delivery.[5–8]

By mimicking or intercepting the key functions of carbohydrates in biological systems, glycosylated nanoparticles hold promise to provide functions such as targeted delivery, inhibition of viral or bacterial infection, and as vaccines.[9–16] Three different approaches have been explored to date for the synthesis of glycosylated nano-assemblies: (1) the conjugation of glycans to preformed nanocarriers;[17] (2) the self-assembly of amphiphilic glycan end-functionalized synthetic macromolecules;[18] and (3) the formation of nanocarriers from macromolecules comprising carbohydrate-based hydrophilic blocks.[19,20] This last approach favours the formation of nanomaterials with highly functionalized inner and outer surfaces. This allows biomolecules to both be located in internal layers and also to better coat the surface of the nano-assemblies, resulting in an enhancement in interactions with biological targets in comparison with the other two approaches.[21]

Block copolymers often have linear-linear architectures because of the synthetic approach that is used to prepare them - most often sequential controlled polymerization. Among alternative architectures, the combination of dendritic and linear blocks opens up new possibilities, in particular for the design of amphiphilic block copolymers with specific morphologies.[22,23] Linear-dendritic block copolymers merge the properties of two different macromolecular structures. On one hand, monodisperse dendrons bring an exact number of peripheral groups that can be tailored in a controlled manner by varying the dendron generation. On the other hand, the linear components are easy to synthesize and to tune in length. The combination of both of these components in a same macromolecule affords advantages including the ability to easily adjust the hydrophilic to hydrophobic ratio (*f*) by modifying the length of the linear block, and the ability of the dendritic block to display ligands in a multivalent manner on the assembly surface where they are readily accessible for binding to proteins or other biological

targets including cells, viruses, and bacteria.

Herein, we report the design of a novel biomimetic system that combines the advantages of the multivalent display of sugars provided by dendrons with the easy self-assembly modulation of amphiphilic copolymers. As a linear block, poly(γ-benzyl-*L*-glutamate) (PBLG) was selected. This hydrophobic polypeptide adopts an α-helical conformation in most environments, and when incorporated into amphiphilic block copolymers has been shown to self-assemble into various morphologies including micelles and vesicles in aqueous solution. A polyester backbone based on 2,2-bis(hydroxymethyl)propionic (bis-HMPA) acid was selected for the dendritic component as it has been found to be non-toxic over a broad range of concentrations when administered intravenously for drug delivery applications.[24–26] It can be readily prepared using a divergent growth strategy,[27,28] and can be functionalized with peripheral amines for further modification with carbohydrates.[17,29]

α-Galactose was chosen as the carbohydrate moiety because of its known immunostimulatory effects.[30] While found in other mammals and many other organisms, terminal α-galactose residues are not found natively in primates.[31] Terminal α-galactose residues are typically a sign of pathogenesis in primates, making their exploitation for immunotherapy highly promising. Thus far, there are very few examples of polymer assemblies incorporating α-galactose.[32] In addition, rather than employing a standard *O*-glycoside, a *C*-glycoside was employed. In biological applications, the native glycosidic bond is labile as it is susceptible to both enzymatic cleavage and non-specific hydrolysis.[33] Although this cleavage is essential for the biological role of carbohydrates, it is often not desirable in biologically active synthetic glycoconjugates as the aglycons and free carbohydrates are inactive individually. The use of *C*-glycosides is a simple approach to overcome this limitation while minimizing structural and conformational perturbations.[33–35] *C*-glycosides have been shown to have similar or better biological activity than their *O*-linked analogues,[36–38] which is proposed to arise from their increased bioavailability. A copper-assisted azide-alkyne cycloaddition (CuAAC) between azide-terminated PBLG of varying lengths and galactose-functionalized dendrons of varying generations with alkyne focal points was used to prepare a small library of linear-dendritic glycopolypeptide mimics. The self-assembly of these new amphiphiles in water was studied in order to investigate the effect of amphiphile architecture and *f* on their aggregation.

Results and discussion

Synthesis of α-galactose-functionalized dendrons

Based on our previous work,[17,39] the reaction of isothiocyanate-functionalized sugars with dendrons bearing peripheral amine groups is an effective method for the synthesis of carbohydrate-functionalized dendrons. Therefore, the first step towards the preparation of the target structures was to prepare an isothiocyanate-functionalized α-galactose. Galactose derivative **1** (Scheme 1), having an azidoethyl substituent at the anomeric position was prepared as previously reported.[40] The acetate groups were then cleaved under Zemplen conditions to afford **2**. The azide functionality of **2** was then cleanly reduced using catalytic hydrogenation to the corresponding amine **3**. Finally, reaction of the amine derivative with thiophosgene in the presence of excess *N*,*N*-diisopropylethylamine (DIPEA) provided the isothiocyanate derivative **4** along with DIPEA salts.

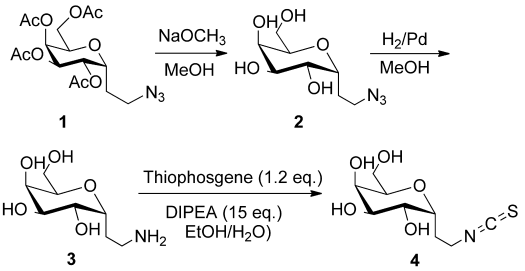

Scheme 1. Synthesis of an isothiocyanate derivative of α-galactose (**4**).

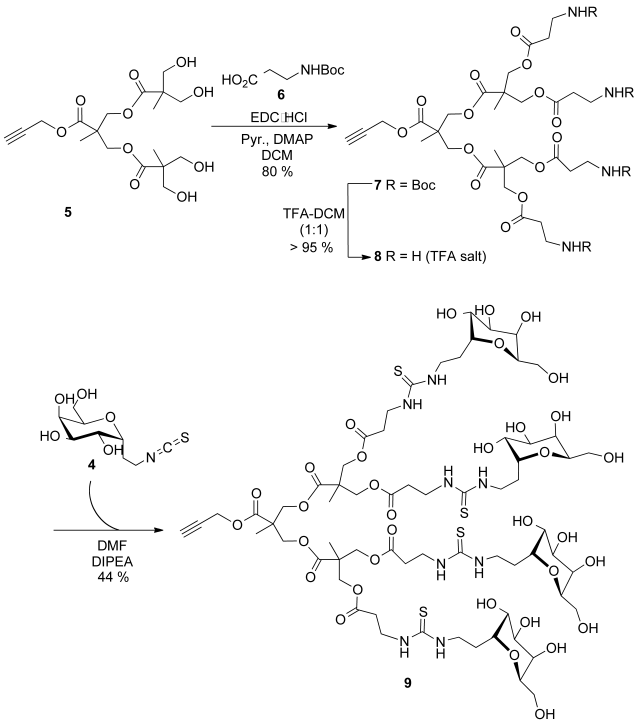

Scheme 2. Synthesis of G2-gal (**9**) from dendron **5** via conversion of the peripheral hydroxyls to amines, then reaction with an isothiocyanate derivative of α-galactose.

This material could be used directly without further purification for functionalization of the dendrons, but analytically pure samples of **4** could also be obtained by chromatography. It was found that unlike previous reports that used thiophosgene in the absence of DIPEA for the activation of amine-functionalized sugars,[17] without DIPEA very low yields of **4** were obtained, likely due to the protonation and inactivation of unreacted amines with the hydrochloric acid formed *in situ*.

Polyester dendrons based on bis-HMPA were synthesized divergently from a focal point propargyl alcohol using a previously reported approach.[41–43] As shown in Scheme 2 for the second generation dendron (G2-OH) **5**, the peripheral alcohol groups were reacted with t-butyloxycarbonyl (Boc)-protected β-alanine (**6**) in the presence of *N*-(3-dimethylaminopropyl)-*N*′-ethylcarbodiimide hydrochloride (EDC·HCl) to provide the Boc-protected dendron **7**. The Boc groups were removed using

trifluoroacetic acid (TFA) to provide dendron **8**. The peripheral amine groups of **8** were then reacted with isothiocyanate **4** in the presence of excess DIPEA, affording the target galactose-functionalized G2 dendron (G2-Gal, **9**). The product was purified by dialysis against *N*,*N*-dimethylformamide (DMF), DMF:pH 6.8

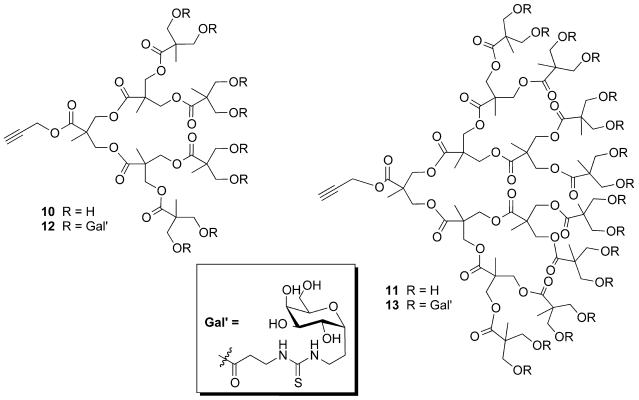

Fig. 1. Chemical structures of the third and fourth generation hydroxyl and galactose-functionalized dendrons.

phosphate buffer 70:30, and finally pure water in order to remove excess unconjugated carbohydrate as well as salts. Starting from the hydroxyl-functionalized dendrons G3-OH (**10**)[43] and G4-OH (**11**)[41] the third (G3-Gal, **12**) and fourth (G4-Gal, **13**) generation analogues (Fig. 1) were prepared by the same procedure (Scheme S1). The yields increased from 44% for G2-gal and 49% for G3-Gal to 64% for G4-Gal. This was attributed to some loss of product during the dialysis of the smaller, lower generation molecules. The molecules were characterized by ^{1}H and ^{13}C NMR spectroscopy, IR spectroscopy, and mass spectrometry (MS). Spectral data were consistent with the expected structures, though mass spectrometry was particularly challenging for the carbohydrate-functionalized dendrons and mainly peaks corresponding to fragments were observed for the higher generations.

Synthesis of PBLG

Following a previously reported approach,[44] ring opening polymerization of ɣ-benzyl-L-glutamate *N*-carboxyanhydride (**14**) was performed using a 1-azido-3-aminopropane initiator to afford α-azido poly(ɣ-benzyl-L-glutamate) (PBLG) (Scheme 3). However, the reaction was performed in CH_2Cl_2 overnight at 10 °C, the low reaction temperature disfavouring the chain-end cyclization.[45] Different degrees of polymerization (DPs) were obtained by varying the ratio of monomer to initiator. This provided PBLG-14, PBLG-28, and PBLG-54, with corresponding DPs of 14, 28, and 54 respectively. These DPs were determined by ^{1}H NMR spectroscopy in 85:15 $CDCl_3$:TFA, based on the relative integrations of the peak at 3.35 ppm, corresponding to the methylene groups adjacent to the amide and azide on the initiator (N_3-C**H**$_2$-CH$_2$-C**H**$_2$-NHR), and the peak at 4.55 ppm corresponding to the α-carbon of the amino acid (CO-C**H**-NH-R) (Fig. S18, ESI). Distinct peaks at ~2100 cm^{-1}, corresponding to azide stretching were also observed in the infrared spectra of these polymers (Figure S19, ESI). Size exclusion chromatography (SEC) in DMF was also performed on these polymers (Figure S20-22, ESI). PBLG-28 and PBLG-54 exhibited monomodal molar mass distributions and low dispersities (*Đ*) of 1.04 – 1.07. On the other hand PBLG-14 exhibited a bimodal distribution. Barz and coworkers recently reported that bimodality was observed in SEC for shorter chains of poly(*N*-ε-benzyloxycarbonyl-L-lysine) due to the coexistence of helical and random coil structures in solution.[46] PBLG undergoes similar conformational phenomena, likely explaining the bimodality in the current case.[47]

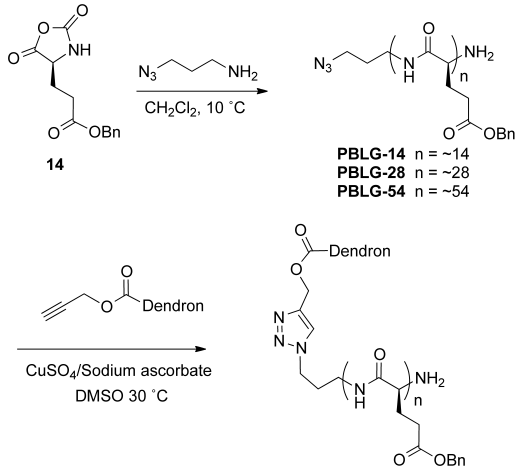

Scheme 3. Synthesis of PBLG *via* ring opening of ɣ-benzyl-L-glutamate *N*-carboxyanhydride initiated by 1-azido-3-aminopropane, followed by copper-assisted coupling to alkyne-functionalized dendrons.

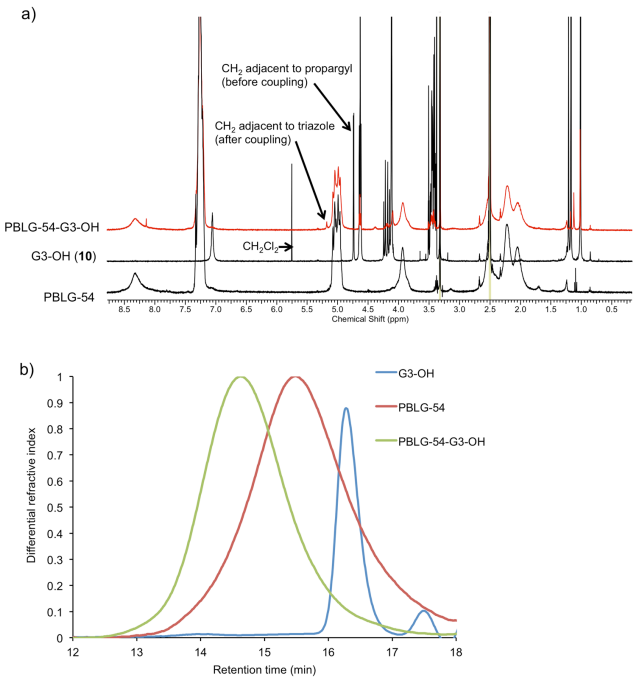

Fig. 2. a) ^{1}H NMR spectra (400 MHz, *DMSO-d*$_6$) of PBLG-54, G3-OH, and PBLG-54-G3-OH showing that the coupling product has peaks corresponding to each component and that the chemical shift of the peak adjacent to the propargyl ester shifted following coupling; b) Overlay of SEC traces for PBLG-54, G3-OH, and PBLG-54-G3-OH showing a shift in the peak retention time of the coupled product and the absence of free dendron.

Synthesis of linear-dendritic block copolymers

Couplings of the azide-terminated PBLGs to the focal point

alkynes of the dendrons were performed using a CuAAC (Scheme 3). DMSO was selected as the solvent and sodium ascorbate as the reducing agent because these conditions have been successfully used to couple linear polysaccharides such as dextran and hyaluronan to PBLG.[19,48] All reagents were used in excess relative to the PBLG, to ensure full conversion of PBLG, as the removal PBLG homopolymer was expected to be challenging. The reaction was first performed to couple PBLG-54 to G3-OH, due to the ease of characterizing the linear-dendron hybrid product PBLG-54-G3-OH by SEC. After stirring overnight at 30 °C, the reaction mixture was transferred to a 50 kg/mol molecular weight cut-off (MWCO) dialysis membrane and dialyzed first against ethylenediaminetetraacetic acid (EDTA), then against pure water in order to remove the copper and ascorbate salts as well as excess dendron. After lyophilization, the product was characterized by ^{1}H NMR spectroscopy, SEC, and IR spectroscopy. As shown in Fig. 2a, an overlay of NMR spectra corresponding to G3-OH, PBLG-54, and PBLG-54-G3-OH shows that characteristic peaks corresponding to both the PBLG-54 and G3-OH are present in the spectrum of the coupled product. In addition, the peak corresponding to the protons adjacent to the alkyne functionality of the dendron (-O-C**H**$_2$-CCH) shifted downfield from 4.74 ppm to 5.19 ppm, indicative of triazole formation. SEC showed a shift in the peak to a shorter elution time and the absence of a peak corresponding to uncoupled G3-OH, again confirming successful coupling and the removal of excess dendron (Fig. 2b). Finally, IR spectroscopy showed complete disappearance of the azide peak at 2100 cm^{-1} (Figure S23, ESI).

Next, these conditions were applied to create a small library of linear-dendritic block copolymers with hydrophilic mass fractions (f) ranging from f = 0.07 for PBLG-54-G3-OH to f = 0.53 for PBLG28-G4-Gal (Table 1), where f is calculated as molar mass of the dendron/(molar mass of dendron + molar mass of PBLG). It should be noted that these f values can be considered as approximations due to the inherent dispersity in chain length of each PBLG as well as the partial hydrophobic character of the polyester dendritic backbone. Nevertheless, they provide a useful comparison between the different systems in this study. As demonstrated above for PBLG-54-G3-OH, in each case characteristic peaks of both the glycodendron and PBLG were observed in the spectra with integrations suggestive of quantitative or near-quantitative coupling, and the characteristic peak corresponding to the protons next to the alkyne functionality shifted downfield as the alkyne was converted to a triazole (Fig. S25-S31, ESI). The disappearance of the azide peak in the IR spectrum was also verified for all compounds (Fig. S23). Unfortunately, the incompatibility of the galactose-functionalized dendrons with SEC in DMF made it impossible to analyze these products by SEC.

Table 1. Summary of the synthesized linear-dendritic block copolymers and their respective hydrophilic mass fractions (f).

	G3-OH	G2-Gal	G3-Gal	G4-Gal
PBLG-14	-	PBLG-14-G2-Gal f = 0.35	-	-
PBLG-28	PBLG-28-G3-OH f = 0.12	PBLG-28-G2-Gal f = 0.21	PBLG-28-G3-Gal f = 0.35	PBLG-28-G4-Gal f = 0.53
PBLG-54	PBLG-54-G3-OH f = 0.07	-	PBLG-54-G3-Gal f = 0.22	-

Self-assembly of linear-dendritic block copolymers

The self-assembly behaviour of the linear-dendritic block copolymers in water was studied by the solvent displacement method. To induce self-assembly, a solution of copolymer in an organic solvent was rapidly injected into water, a non-solvent for PBLG, or water was added dropwise to the copolymer solution to induce nanoprecipitation. The organic solvent was then removed by dialysis. With the aim of determining the optimal conditions to form well-defined and reproducible assemblies, several parameters were tuned including identity of the organic solvent, the order of solvent addition, and the rate of addition of non-solvent. The adjustment of all these parameters allows exploration of the thermodynamic and kinetic conditions the most appropriate for the system to obtain stable nanoparticles of controlled size and shape.[49,50] The resulting assemblies were characterized by transmission electron microscopy (TEM) (Fig. 3) and either single-angle or multi-angle dynamic light scattering (DLS) (Table 2). DLS analysis indicated that these systems exhibit only one relaxation time and consequently a monomodal distribution. In addition, the linear variation of the relaxation frequency Γ versus the squared scattering vector q^2 passing through the origin is the hallmark of a translational diffusive process, confirming the presence of spherical objects with a pure diffusive mode (Fig. 4). Autocorrelation functions and relaxation time distributions are provided for all the samples in the ESI (Figures S32 and S33).

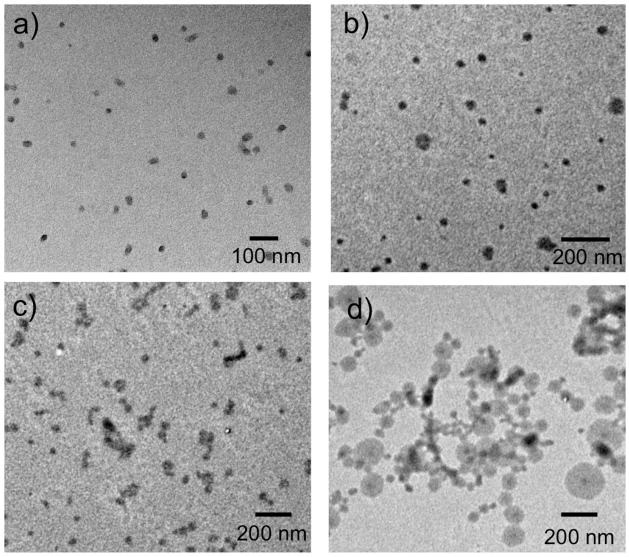

Fig. 3. TEM images of assemblies: a) PBLG-28-G4-Gal alone obtained by fast injection of a DMSO solution of copolymer into water; b) PBLG-28-G4-Gal + 5 wt% PBLG-28 obtained by fast injection of a DMSO solution of copolymer into water; c) PBLG-28-G3-OH obtained by fast injection of a DMSO solution of copolymer into water; d) PBLG-54-G3-OH obtained by slow (8 mL/h) injection of water into a DMSO solution of copolymer. The samples are all unstained.

Table 2. Hydrodynamic diameters and polydispersity indices (PDIs) measured by DLS of the assemblies formed from PBLG-28-G4-Gal as a function of the assembly procedure. * indicates values obtained multi-angle analysis.

Sample	d_H (nm)	PDI
PBLG-28-G4-Gal (DMSO into water, fast)	40*	0.25
PBLG-28-G4-Gal + 5 wt% PBLG-28 (DMSO into water, fast)	50	0.15
PBLG-28-G4-Gal (DMF into water, fast)	80*	0.17

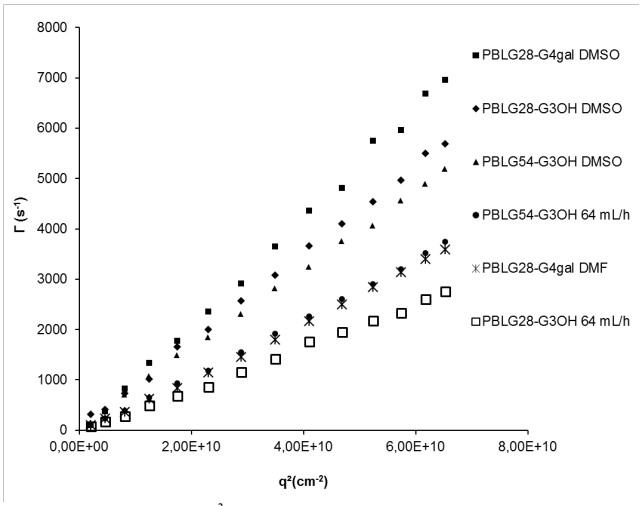

Fig. 4. Plot of Γ versus q^2 for the assemblies in water at a concentration of 1 mg/mL at angles between 20 and 150°.

For PBLG-28-G4-Gal (f = 0.53), an optically clear solution was obtained when a dimethyl sulfoxide (DMSO) solution of copolymer was rapidly injected into water. DLS measurements indicated that the resulting assemblies had a hydrodynamic diameter (d_H) of 40 nm with a relatively low PDI of 0.25. TEM images suggested a micellar morphology with a somewhat smaller diameter on the order of ~20 nm (Fig. 3a). Despite the rod-like character of the PBLG segment, which is known to induce flat interfaces,[51] this micellar morphology is likely favoured by the interfacial curvature imposed by the dendron. A similar tendency for the formation of spherical micelles was also previously observed for amphiphilic copolymers composed of PBLG conjugated to multiple arms of linear dextran or hyaluronan.[20] Spherical micelles were also obtained using mannose-terminated polysarcosine-PBLG block copolymers, though in this case a ~10:1 molar ratio of the hydrophilic sarcosine to hydrophobic γ-benzyl-*L*-glutamate monomers was used.[52] Micelles have also been prepared from poly(ethylene oxide)-PBLG block copolymers at high hydrophilic:hydrophobic ratios.[53] In contrast, fully linear diblock copolymers of PBLG and poly(galactosylated propargylglycine) with a similar hydrophilic weight fraction to PBLG-28-G4-Gal (0.55) formed vesicles.[10]

The larger diameter measured in solution by DLS versus TEM in the solid state can likely be attributed to the hydration shell associated with the carbohydrates on the micelle periphery. Given an expected end-to-end distance for PBLG-28 of ~4.2 nm based on the standard α-helical pitch, as well as an additional 2-3 nm for the dendron block (Fig. 5d), the sizes of these assemblies observed by TEM suggest a true micellar structure. Through encapsulation of the fluorescent probe Nile red, the critical aggregation concentration was found to be ~0.3 g/L (ESI, Figure S37). This value lies within the upper range of those obtained from polymeric amphiphiles, and might be attributed to the relatively low molar mass of the amphiphile.

When 5 wt% of PBLG-28 homopolymer was added, an increase in d_H to 50 nm (PDI = 0.15) was observed, but TEM imaging indicated that solid particles were retained (Fig. 3b). This suggests that the PBLG homopolymer was incorporated into the micelle core, enlarging it. Changing the organic solvent from DMSO to DMF also resulted in an increase in d_H, in this case to 80 nm (PDI = 0.17), while retaining the solid particle morphology (Figure S34, ESI). Under such kinetically controlled conditions, the slightly higher solubility of DMSO in water compared to DMF may allow a slower dispersion of DMF polymer solutions, resulting in larger particle sizes. Changing the order of solvent addition such that water was added to the organic solvent led to the formation of macroscopic aggregates. It was also found that the assemblies prepared by the rapid addition or organic solvent to water were very sensitive to ionic strength, with even low (10 mM) concentrations of various buffers such as pH 7.4 phosphate or 4-(2-hydroxyethyl)piperazine-1-ethanesulfonate (HEPES) buffers leading to gradual precipitation of the micelles over a period of ~30 min.

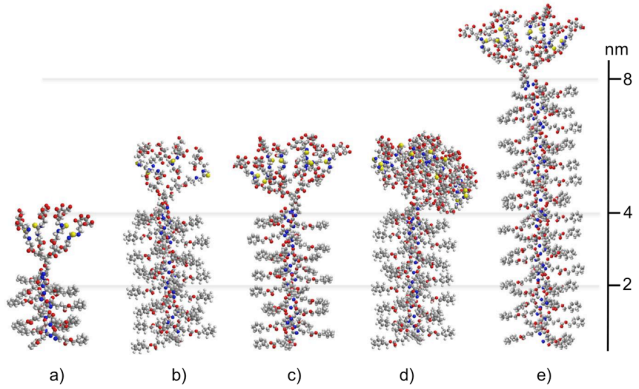

Fig. 5. Chem3D models of the linear-dendritic block copolymers: a) PBLG-14-G2-Gal; b) PBLG-28-G2-Gal; c) PBLG-28-G3-Gal; d) PBLG-28-G4-Gal; e) PBLG-54-G3-Gal.

Turbid solutions of macroscopic aggregates were obtained from the rapid injection of both DMSO and DMF solutions with PBLG-14-G2-Gal, PBLG-28-G2-Gal, PBLG-28-G3-Gal and PBLG-54-G3-Gal. Changing the order of addition, the flow rate or the solvent did not noticeably affect the turbidity. Direct dissolution of copolymer into water also did not result in controlled self-assembly of any of these molecules. All these experiments evidenced that the self-assembly of such rod-dendron shape copolymers (PBLG behaving as a rod) is rather complex. During solvent displacement, the rod-like PBLG tends to assemble in a lamellar manner with a flat interface while the dendrons, having an intrinsic cone-shape, force the interface to curve between the two blocks. Such conformational constraints have been explored both in bulk[54] and in solution[20,55] and have been show to significantly influence the phase diagrams of amphiphilic block copolymers.[56]

In order to gain some insight into this self-assembly behaviour,

simple three-dimensional models were generated using Chem3D software with an MM2 force field for the energy minimization (Fig. 5). Although these models do not take into account the expected hydration spheres of the carbohydrates, they provide information on the relative dimensions spanned by each block. The length of the PBLG increases linearly by 5.4 Å every 3.6 amino acids, the known pitch of an α-helix. In contrast, in dendrimer growth, the available volume grows proportionally to the cube of its radius while the number of monomer units increases exponentially with each generation.[57] As shown in Fig. 5b-d, this results in the dendrimer becoming more compact while occupying a modestly increasing volume. In addition, while the hydrophilic fractions of these amphiphiles may be suitable for their assembly into morphologies such as vesicles, the curvature induced by the cone-shaped dendrons, combined with the rigid conformation of the PBLG may prevent the formation of lamellar phases. This may explain the propensity of many of these amphiphiles to aggregate macroscopically rather than assemble into well-defined nanostructures. Deming and coworkers have investigated the influence of the conformation of the hydrophilic block on the self-assembly of α-helical poly(L-leucine)-based amphiphilic block copolymers.[32] They found that vesicle formation was possible when the α-galactose-functionalized hydrophilic block assumed a random coil conformation, whereas when the α-galactose-functionalized hydrophilic block had an α-helical conformation, micro-sized irregular and platelike aggregates were observed. This was attributed to the inability of the rigid hydrophilic domains to effectively solubilize and stabilize the membranes against further aggregation, as well as the lack of flexibility required for the formation of membranes. Such factors may also be involved in the aggregation of the copolymers in the current study. Of the investigated amphiphilies, only PBLG-28-G4-Gal has sufficiently high curvature and hydrophilic fraction to allow for micelle formation, and even this is a fragile balance as indicated by the tendency of these assemblies to precipitate in salt solutions.

The self-assembly of the non-carbohydrate linear-dendritic copolymers was also studied. Interestingly, PBLG-28-G3-OH and PBLG-54-G3-OH, despite their low hydrophilic fractions (respectively f = 0.12 and f = 0.07) were able to assemble as nano-objects, forming optically clear suspensions in water (Table 3). CACs measured using the Nile red method were ~0.10 and 0.080 g/L for PBLG-28-G3-OH and PBLG-54-G3-OH respectively (Figure S37), which are lower than that of PBLG-28-G4-Gal and are in line with the relative f values of these amphiphiles. Assemblies obtained by the rapid injection of a DMSO solution of copolymer into water were solid aggregates resembling those obtained from PBLG-28-G4-Gal by the same assembly method in both size and morphology (Fig. 3c and S36a). As shown in Table 3, an increase in d_H was observed with the decrease in the flow rate when injecting water into the DMSO solution of the copolymer. TEM revealed the coexistence of smaller assemblies that were likely micelles with larger spherical objects (Figs. 3d, S35, S36b). These images strongly resemble those obtained for assemblies of copolymers based on linear PBLG and branched dextran mixed with PBLG homopolymer.[55] These assemblies were proposed to be disk-like morphologies that may be intermediates in the micelle to vesicle transition,[58] and may arise from an initial lamellar growth that becomes limited due to the strong curvature of the branched block. This is also likely the case for the current linear-dendron copolymers.

Table 3. Hydrodynamic diameters of the assemblies formed from PBLG-28-G3-OH and PBLG-54-G3-OH as a function of the assembly procedure. * indicates values obtained multi-angle DLS.

Order of injection		DMSO into Water Fast		Water into DMSO Fast		Water into DMSO 64 mL/hr		Water into DMSO 8 mL/hr	
Sample	***f***	**d_H (nm)**	**PDI**	**d_H (nm)**	**PDI**	**d_H (nm)**	**PDI**	**d_H (nm)**	**PDI**
PBLG-28-G3-OH	0.12	49*	0.17	56	0.16	104*	0.09	-	-
PBLG-54-G3-OH	0.07	54*	0.20	40	0.14	77*	0.17	175	0.18

Conclusions

A *C*-linked α-galactose derivative functionalized with an isothiocyanate was synthesized and conjugated to the peripheries of second through fourth generation polyester dendrimers having focal point alkynes. PBLGs with terminal azides and DPs of 14, 28, and 54 were synthesized by ring-opening polymerization and were coupled to the dendrons to afford a small library of linear-dendritic block copolymers with varying hydrophilic mass fractions from 0.07 to 0.54. The self-assembly of the amphiphiles in water was studied using a solvent exchange (nanoprecipitation) method. It was found that PBLG-28-G4-Gal assembled via the rapid injection of a DMSO solution into water to form micelles with d_H of 40 nm. The d_H could be increased and tuned by changing the organic solvent to DMF or by adding PBLG homopolymer. All other linear-dendritic block copolymers with lower f, prepared from α-galactose-functionalized dendrons formed macroscopic aggregates by all investigated methods. This was attributed to the overall conformational rigidities of the molecules as well as their architectures. While the densely branched dendrons which impart interfacial strong curvature favouring micellar morphologies, the rod-like PBLG favours competing lamellar-type packing. Only in the case of PBLG-28-G4-Gal was the volume of the dendritic block sufficient to force PBLG into a micellar morphology. On the other hand, copolymers PBLG-28-G3-OH and PBLG-54-G3-OH, containing a hydroxyl-functionalized dendron without galactose units assembled to form nanoaggregates despite their much lower calculated hydrophilic mass fractions. This might be related to the less sterically congested dendritic blocks in these structures, which affords increased flexibility in the self-assembly process; however, the reasons for this are unclear. Overall, this work provides the first example of nano-assemblies densely functionalized with *C*-linked α-galactose. While the aggregation of the assemblies in buffers prevents the assessment of their lectin binding affinities, these new nanomaterials can potentially serve as platforms for the development of immunotherapeutics. It is anticipated that in the future, such aggregation can be overcome by increasing the hydrophilic volume fraction and flexibility of the copolymer. This can be achieved by either changing the hydrophobic block or adding additional hydrophilic components to the copolymer.

Experimental

General procedures and materials

Galactose **1**,[40] 1-azido-3-aminopropane,[44] and hydroxyl-functionalized dendrons,[41,43] were synthesized and purified as previously reported. ɣ-Benzyl-L-glutamate *N*-carboxyanhydride was obtained from Isochem S. A. S. (Very le Petit, France) and stored at -30 °C in a glovebox. All manipulations of this monomer were performed in a glovebox. All other chemicals were obtained from commercial suppliers and used as received unless otherwise noted. Triethylamine (NEt_3), DIPEA, CH_2Cl_2 and pyridine were distilled from CaH_2 before use. Anhydrous tetrahydrofuran (THF) and DMF were obtained from an Innovative Technology (Newburyport, USA) solvent purification system based on aluminium oxide columns. Flash chromatography was performed using SiliaFlash P60 (Silicycle, Quebec City, Canada). Thin layer chromatography (TLC) was performed using Merck silica gel plates (60-mesh F_{254} plates, EMD Millipore) and visualized using either UV light (254 nm), potassium permanganate stain or Hanessian's stain. Dialyses were performed using Spectra/Por regenerated cellulose membranes (Spectrum Labs) with 1 kg/mol, 2 kg/mol, or 50 kg/mol MWCO. NMR spectra were recorded at ambient temperature on Bruker Advance 400, Varian Inova 400 MHz, or Varian Inova 600 MHz spectrometers. NMR chemical shifts (δ) are reported in ppm and are calibrated against residual solvent signals of $CDCl_3$ (δ 7.26) or DMSO-d_6 (δ 2.50) or CD_3OD (δ 3.30). Fourier transform infrared (IR) spectroscopy measurements were performed on either films from CH_2Cl_2, $CHCl_3$ or methanol on NaCl plates, as KBr pellets, or in the attenuated total reflection (ATR) mode using a Bruker Tensor 27 instrument. Matrix-assisted laser desorption ionization time of flight (MALDI-TOF) mass spectrometry (MS) was performed using either an AB Sciex TOF/TOF instrument while electron impact (EI) and chemical impact (CI) MS were performed on a Finnigan MAT 8200. TEM images were recorded on a Hitachi H7650 microscope working at 80 kV. The samples were sprayed on carbon-coated grids. SEC data for PBLGs were obtained using an Acquity Advanced Polymer Chromatography System (Waters) equipped with an Acquity APC XT column for extended temperature organic-based separations (4.6 x 150 mm) and an Acquity Refractive Index detector. The calibration was performed using polystyrene standards. Samples (5 mg/mL) were dissolved in DMF and were run at a flow rate of 0.5 mL/min at 55 °C. The SEC overlay data presented in Fig. 2b were obtained using a Waters 2414 pump equipped with a Wyatt Optilab T-rEX Refractive Index Detector and two PLgel 5 µm mixed-D (300mm x 7.5mm) columns and a guard column connected in series (Varian Canada Inc., Mississauga, ON). Samples (5 mg/mL) dissolved in the eluent (10 mM LiBr and 1% (vol/vol) NEt_3 in DMF at 85 °C) were injected at a flow rate of 1 mL/min.

1-azido-2-(α-D-galactopyranosyl)-ethane (2)

Acetate protected azido galactose **1**[40] (3.6 g, 8.91 mmol) was dissolved in methanol (25 mL) and 5 mL of 1 M $NaOCH_3$ in methanol was added. The reaction mixture was stirred under nitrogen at room temperature for 1 hour. Methanol-rinsed DOWEX-30X resin (~ 100 mg) was added to neutralize the reaction, and the reaction mixture was stirred for an additional 5 minutes. After checking the pH to ensure neutrality, the reaction was diluted with water and filtered. The filtrate was concentrated to provide 2.0 g of **2** as a clear oil, which was taken to the next step without further purification. ^{1}H NMR (600 MHz, *CD_3OD*): δ_{ppm} 4.04-3.98 (m, 1H), 3.88-3.84 (m, 1H), 3.83-3.81 (m, 1H), 3.64-3.57 (m, 4H), 3.42-3.24 (m, 2H), 1.92-1.82 (m, 1H), 1.83-1.76 (m, 1H); ^{13}C NMR (100 MHz, *CD_3OD*): δ_{ppm} 74.4, 73.3, 72.0, 70.3, 70.1, 62.4, 49.5, 25.8; IR ν_{max} (film from MeOH): 3620, 2297, 1541 cm^{-1}.

2-(α-D-galactopyranosyl)-ethylamine (3)

Azide **2** (600 mg, 2.57 mmol) was dissolved in methanol (5 mL) under a nitrogen atmosphere. After the flask was thoroughly purged, Pd/C catalyst (60 mg of 10 wt% Pd) was added. The reaction mixture was purged with hydrogen gas and equipped with a hydrogen balloon. It was then stirred for 4 hours (TLC indicated reaction completion), then exposed to the atmosphere and filtered through a celite pad. The pad was washed extensively with methanol and water, and the combined filtrates were concentrated *in vacuo* and then lyophilized to provide 467 mg of a white amorphous solid in 87 % overall yield from **1** over the two steps. This material could then be precipitated from isopropanol/ether with 85 % mass recovery to provide an analytically pure sample. White amorphous solid. Rf = 0.45 (4:1, EtOAc-MeOH); ^{1}H NMR (600 MHz, *CD_3OD*): δ_{ppm} 4.03 (ddd, *J* = 10.8, 5.6, 3.7 Hz, 1H), 3.90 (dd, *J* = 2.9, 2.9 Hz, 1H), 3.86 (dd, *J* = 9.9, 6.1 Hz, 1H), 3.82-3.77 (m, 1H), 3.73-3.69 (m, 1H), 3.67-3.62 (m, 2H), 2.83-2.71 (m, 2H), 1.92-1.83 (m, 1H), 1.76-1.69 (m, 1H); ^{13}C NMR (150 MHz, *CD_3OD*): δ_{ppm} 74.0, 73.3, 71.7, 70.2, 69.8, 62.3, 49.3, 25.4; IR ν_{max} (film from MeOH): 3368, 2920, 1560 cm^{-1}; EI (HRMS): Calculated for $C_8H_{18}NO_5$ $(M+H)^+$: 208.1185. Found: 208.1183.

2-(α-D-galactopyranosyl)-ethylisothiocyanate (4)

Amine **3** (2.0 g, 7.5 mmol) was dissolved in a mixture of absolute ethanol (100 mL) and deionized water (24 mL) under a nitrogen atmosphere. DIPEA (5.8 g, 7.8 mL, 45 mmol) was added and the reaction mixture was cooled to 0 ºC. Thiophosgene (1.3 g, 0.86 mL, 11 mmol) was added, and then the ice bath removed and the reaction mixture stirred for 1.5 hours at ambient temperature. The solvent was then removed *in vacuo* and the orange residue was co-evaporated twice with toluene. The resulting liquid was triturated with diethyl ether and benzene successively, and dried *in vacuo*, providing 3.2 g of a thick brown gel containing the title compound and DIPEA salts. A small portion was purified by preparative TLC (10 % methanol in ethyl acetate, five elutions) to provide a pure sample of **4** as a colorless gel for characterization. Yield = 60 %; Rf = 0.8, (77:23, EtOAc-MeOH); ^{1}H NMR (400 MHz, *DMSO-d_6*): δ_{ppm} 4.82 (d, *J* = 4.9 Hz, 1H), 4.58 (d, *J* = 5.3 Hz, 1H), 4.41 (t, *J* = 5.4 Hz, 1H), 4.31 (d, *J* = 4.9 Hz, 1H), 3.79 (ddd, *J* = 11.0, 5.2, 3.6 Hz, 1H), 3.69-3.62 (m, 4H), 3.53-3.36 (m, 4H), 1.98-1.87 (m, 1H), 1.84-1.74 (m, 1H); ^{13}C NMR (100 MHz, *DMSO-d_6*): δ_{ppm} 185.1, 73.2, 70.7, 70.2, 68.2, 68.0, 60.2, 41.8, 25.5; IR ν_{max} (film from MeOH): 3270, 2928, 2360, 2110, 1520 cm^{-1}; CI (HRMS): Calculated for $C_9H_{16}NO_5S$ $(M+H)^+$: 250.0749; Observed 250.0752.

Second generation Boc-protected dendron (7) and representative procedure for the preparation of the Boc-protected dendrons

Dendron **5** (4.25 g, 10.5 mmol, 1.0 equiv.)[43] and Boc-protected β-alanine (**6**) (15.9 g, 84.2 mmol, 8.0 equiv.), were dissolved in distilled pyridine under a nitrogen atmosphere (8.4 mL, 10 equiv.). EDC·HCl (13.1 g, 84.2 mmol, 8.0 equiv.) and 4-(dimethylamino)pyridine (DMAP) (10.27 g, 84.2 mmol, 8 equiv.) were then added. Anhydrous CH_2Cl_2 (50 mL) was added and the mixture was stirred at room temperature for 36 hours. The solution was then diluted with 100 mL of CH_2Cl_2, and sequentially washed with H_2O (1 x 50 mL), 1M HCl (3 x 50 mL), 1 M Na_2CO_3 (2 x 50 mL), and brine (1 x 50 mL). The organic phase was then dried with $MgSO_4$, filtered and concentrated *in vacuo*. Column chromatography (1.5:1, hexanes:ethyl acetate) of the resulting residue provided dendron **7** as a white, amorphous solid (9.1 g, 80% yield). ^{1}H NMR (400 MHz, *CDCl$_3$*): δ_{ppm} 5.18 (br s, 1H), 4.74 (d, *J* =2.3 Hz, 2H), 4.31-4.10 (m, 12H), 3.41-3.35 (m, 8H), 2.54 (t, *J* = 6.6 Hz, 8H), 1.47-1.40 (m, 36H), 1.29 (s, 6H), 1.26 (s, 3H); ^{13}C NMR (100 MHz, *CDCl$_3$*): δ_{ppm} 171.8, 171.3, 155.7, 79.2, 76.9, 75.6, 65.5, 64.8, 60.2, 52.8, 46.5, 46.3, 36.0, 34.3, 33.8, 28.2, 20.9, 17.7, 17.4; IR ν_{max} (film from $CHCl_3$): 3370, 2970, 2924, 2110, 1735, 1703, 1508 cm^{-1}; MALDI-TOF Calcd for $C_{50}H_{80}N_4O_{22}Na$ $(M+Na)^+$: 1111.6. Found: 1111.5.

Second generation amine-functionalized dendron (trifluoroacetate salt) (8) and representative procedure for the synthesis of amine-functionalized dendrons

Dendron **7** (0.25 g, 0.23 mmol) was dissolved in 1 mL of 1:1 TFA:CH_2Cl_2 and the solution was stirred under a nitrogen atmosphere at room temperature for 2 hours. The solvent was removed *in vacuo* to provide dendron **8** as a light brownish viscous oil (0.26 g, 98% yield). The material was stored at -4 ºC. ^{1}H NMR (400 MHz, *CD$_3$OD*) δ_{ppm} 4.79 (d, *J* = 2.3 Hz, 2H), 4.35-4.26 (m, 12H), 3.22 (t, *J* = 6.4 Hz, 8H), 3.02 (t, *J* = 2.3 Hz, 1H), 2.79 (t, *J* = 7.0 Hz, 8H), 1.33 (s, 3H), 1.29 (s, 6H); ^{13}C NMR (100 MHz, *CD$_3$OD*): δ_{ppm} 173.6, 171.9, 162.5 (q, J = 36 Hz), 118.0 (q, J = 290 Hz), 78.6, 77.2, 67.1, 54.0, 47.8, 39.5, 36.4, 34.8, 32.2, 26.8, 26.2, 18.1, 18.0; IR ν_{max} (film from MeOH): 3244, 2982, 2916, 1733, 1676 cm^{-1}; MALDI-TOF MS Calcd for $C_{30}H_{48}N_4O_{14}Na$ $(M+Na)^+$: 711.3. Found: 711.3.

Second generation α-galactose-functionalized dendron (9) and representative procedure for the synthesis of galactose-functionalized dendrons

Dendron **8** (300 mg, 0.26 mmol) was dissolved in 5 mL of anhydrous DMF under nitrogen. Isothiocyanate **4** (crude product containing 780 mg, 3.1 mmol, 12 equiv. based on ^{1}H NMR spectroscopy), was dissolved in DMF (12 mL) under nitrogen. Freshly distilled DIPEA (3.5 mL, 20 mmol) was added to the isothiocyanate solution and the resulting solution was transferred to the solution of dendron via cannula. The reaction mixture was stirred at ambient temperature for 24 hours, then the temperature was increased to 35 ºC for an additional 48 hours. The solution was then concentrated to dryness and triturated with diethyl ether and dichloromethane successively to provide 1.6 g of crude material. This material was dissolved in DMF (12 mL) and dialysed against DMF (1 kg/mol MWCO) for 12 hours. The dialysis solution was then changed to 70:30 DMF:pH 6.8 phosphate buffer (100 mM)) and the product was dialysed for an additional 12 hours. Finally, the product was dialysed against pure water for 4 hours, and then lyophilized to afford dendron **9** as an off-white solid (190 mg, 44% yield). ^{1}H NMR (400 MHz, *DMSO-d$_6$*): δ_{ppm} 7.58-7.48 (m, 2.5H), 7.44-7.38 (m, 2.5H), 4.76 (d, *J* = 4.5 Hz, 2H), 4.73 (d, *J* = 1.8 Hz, 4H), 4.61 (d, *J* = 4.8 Hz, 4H), 4.53 (m, 4H), 4.36 (dd, *J* = 9.4, 5.0 Hz, 4H), 4.27-4.08 (m, 16H), 3.82-3.75 (m, 4H), 3.74-3.70 (m, 4H), 3.69-3.62 (m, 4H), 3.60-3.39 (m, 20H), 2.67, (t, J = 7.8 Hz, 1H), 2.57 (t, *J* = 6.5 Hz, 8H), 1.87-1.59 (m, 8H), 1.20-1.15 (m, 9H); IR ν_{max} (film from MeOH): 3281, 2968, 2359, 1761, 1734, 1670, 1560, 1468 cm^{-1}; MALDI-TOF MS: Calcd for $C_{66}H_{108}N_8O_{34}S_4Na$ $(M+Na)^+$: 1707.6. Found: 1707.3.

Synthesis of PBLG-28 and representative procedure for the synthesis of azide-terminated PBLG

ɣ-Benzyl-L-glutamate *N*-carboxyanhydride (**14**) (4.0 g, 15 mmol, 28 equiv.) was weighed under pure argon in a glovebox, introduced into a flame-dried Schlenk tube, and dissolved in 40 mL of anhydrous CH_2Cl_2. The solution was stirred for 10 minutes and then 1-azido-3-aminopropane (54 mg, 0.54 mmol, 1.0 equiv.) was added using a nitrogen purged syringe. The reaction mixture was stirred overnight at 10 °C. Precipitation in cold diethyl ether, followed by drying under high vacuum provided PBLG-28 (2.5 g, 76% yield). ^{1}H NMR (400 MHz, 85/15 *CDCl$_3$/TFA*): δ_{ppm} 7.85-7.80 (m, 28H), 7.36-7.21 (m, 173H), 5.15-5.00 (m, 57H), 4.60 (br s, 28H), 3.40-3.25 (m, 4H), 2.65-2.40 (m, 55H), 2.20-1.70 (m, 57H). IR ν_{max} (ATR): 3293, 2997, 2096, 1728, 1648, 1545, 1452 cm^{-1}. SEC: M_n = 18400 g/mol, $Đ$ = 1.07.

Synthesis of PBLG-28-G2-Gal and general procedure for the synthesis of linear-dendritic block copolymers

Dendron **9** (30 mg, 0.018 mmol, 1.1 equiv.), PBLG-28 (100 mg, 0.016 mmol, 1.0 equiv.), and sodium ascorbate (12.6 mg, 0.064 mmol, 2 equiv.) were dissolved in 2 mL of DMSO in a Schlenk tube at 30 °C. $CuSO_4$ (8.0 mg, 0.032 mmol, 4 equiv.) was then added and the reaction mixture was stirred overnight at 30 °C. It was then dialyzed against a solution of ethylenediaminetetraacetic acid (EDTA) (~1 g/L, pH 7) for 24 hours and then deionized water for 48 hours using a 50 kg/mol MWCO membrane. The product was obtained by lyophilization (101 mg, 80% yield). ^{1}H NMR (400 MHz, DMSO-*d$_6$*): δ_{ppm} 8.35-8.05 (m, 23H), 7.30-7.15 (m, 140H), 5.15 (br s, 2H), 5.10-4.85 (m, 56H), 4.35-3.75 (m, 44H), 3.65-3.40 (m, 15H), 2.40-1.75 (m, 94H), 1.15-1.01 (m, 9H). IR ν_{max} (ATR): 3292, 2940, 1730, 1651, 1544, 1453.

Self-assembly

The copolymer was dissolved in DMSO or DMF at a concentration of 10 mg/mL. Different processes for solvent displacement were then tested in order to optimize the resulting nanoparticle formation. For the fast injection of the organic solvent into water, the solution was heated to 50 °C and then rapidly injected into stirring deionized water (already heated to 50 °C) to reach a final concentration of 1 mg/mL. For the addition of water into organic solvent, either the water was injected rapidly into a stirring solution of the copolymer in organic solvent or a syringe pump was used for the injection of

water into DMSO at controlled flow rates. In each case, the organic solvent was then removed by dialysis against water for two days (MWCO 2.5 kg/mol) changing the medium every 4 hrs during the day (3 times per day).

Dynamic light scattering (DLS)

Single-angle DLS was performed on a ZetaSizer Nano ZS instrument with detection at 90° (Malvern, UK). Samples were analyzed at room temperature at a concentration of ~ 1 mg/mL. For multi-angle light scattering, measurements were performed with an ALV/CG-3 laser compact goniometer, which consists of a 22 mW HeNe linear polarized laser operating at wavelength of 632.8 nm and a goniometer to cover a scattering angle range from $\theta = 20°$ to 150° corresponding to a scattering vector $q = 4.6 \times 10^{-3}$ nm^{-1} to 2.55×10^{-2} nm^{-1}, and a thermostated bath controller (20 °C). The autocorrelation functions ($g_1(t)$) were analyzed in terms of relaxation time distribution (τ) (Equation 1) according to the REPES method.[59]

$$g_1(t) = \int A_{(\tau)} \exp\left(\frac{-t}{\tau}\right) d\tau \quad \text{(Equation 1)}$$

Hydrodynamic radius (R_H) was estimated using the Stokes-Einstein relation (Equation 2), where D_0 is diffusion coefficient, η_s is the viscosity of the solvent (water), T is absolute temperature and k_B is the Boltzmann constant. D_0 was determined from the slope of the q^2 dependence of frequency ($\Gamma = 1/\tau$, with τ is relaxation times).

$$R_H = \frac{k_B T}{6\pi\eta_s D_0} \quad \text{(Equation 2)}$$

Measurement of the critical aggregation concentration (CAC)

Micelles were prepared as described above. Nile red (0.94 mg, 3.0 µmol) was dissolved in 9 mL of CH_2Cl_2 and 0.1 mL of this solution was added to a series of vials. The CH_2Cl_2 was removed under a stream of nitrogen. A series of concentrations of the micelle suspension ranging from to 2 mg/L to 1000 mg/L was prepared by serial two-fold dilutions. The micelle suspensions were added to the vials containing Nile red and were allowed to equilibrate with stirring overnight. The fluorescence spectra were obtained on a Varian Cary Eclipse fluorescence spectrometer from Agilent Technologies. An excitation wavelength of 550 nm was used for Nile red and the emission spectra were recorded from 565 to 700 nm. The emission intensity at maximum of excitation was recorded for each micelle concentration. The CAC was determined as the concentration at the intercept of the lines for the two linear regions of the obtained graphs.

Acknowledgements

We thank the Natural Sciences and Engineering Council of Canada Discovery Grant program for funding this work. Aneta Borecki is thanked for acquiring SEC data. The Research Network Program on Precision Polymer Materials from ESF is acknowledged. CNRS funding, via IUPAC Project PAC-POL-10-02-16, is gratefully acknowledged.

Notes and references

[a] *Université de Bordeaux/IPB, ENSCBP; CNRS, Laboratoire de Chemie des Polymères Organique (LCPO), UMR 5629, 16 avenue Pey Berland, F-33600, Pessac, France. E-mail: lecommandoux@enscbp.fr*
[b] *Department of Chemistry, The University of Western Ontario, 1151 Richmond Street, London, Canada, N6A 5B7; E-mail: egillie@uwo.ca*
[c] *current address : CNRS, Laboratoire de Chimie de Coordination (LCC), UPR8241, 205 route de Narbonne, F-31077, Toulouse, France*
[d] *Department of Chemical and Biochemical Engineering, The University of Western Ontario, 1151 Richmond St., London, Canada, N6A 5B9*
† Electronic Supplementary Information (ESI) available: Additional synthesis procedures, NMR spectra, IR spectra, SEC data, DLS data, additional TEM images. See DOI: 10.1039/b000000x/

1 F. S. Bates, *Science*, 1991, **251**, 898–905.
2 L. Zhang and A. Eisenberg, *Science*, 1995, **268**, 1728–1731.
3 H.-C. Kim, S.-M. Park and W. D. Hinsberg, *Chem. Rev.*, 2009, **110**, 146–177.
4 D. E. Discher and A. Eisenberg, *Science*, 2002, **297**, 967–973.
5 Z. L. Tyrrell, Y. Shen and M. Radosz, *Prog. Polym. Sci.*, 2010, **35**, 1128–1143.
6 A. Rösler, G. W. M. Vandermeulen and H.-A. Klok, *Adv. Drug Deliv. Rev.*, 2001, **53**, 95–108.
7 C. Deng, Y. Jiang, R. Cheng, F. Meng and Z. Zhong, *Nano Today*, 2012, **7**, 467–480.
8 P. Tanner, P. Baumann, R. Enea, O. Onaca, C. Palivan and W. Meier, *Acc. Chem. Res.*, 2011, **44**, 1039–1049.
9 G. Huang, F. Cheng, X. Chen, D. Peng, X. Hu and G. Liang, *Curr. Pharm. Des.*, 2013, **19**, 2454–2458.
10 J. Huang, C. Bonduelle, J. Thévenot, S. Lecommandoux and A. Heise, *J. Am. Chem. Soc.*, 2012, **134**, 119–122.
11 M. Marradi, F. Chiodo, I. García and S. Penadés, *Chem. Soc. Rev.*, 2013, **42**, 4728–4745.
12 I. García, M. Marradi and S. Penadés, *Nanomed.*, 2010, **5**, 777–792.
13 J. Rieger, H. Freichels, A. Imberty, J.-L. Putaux, T. Delair, C. Jérôme and R. Auzély-Velty, *Biomacromolecules*, 2009, **10**, 651–657.
14 A. L. Parry, N. A. Clemson, J. Ellis, S. S. R. Bernhard, B. G. Davis and N. R. Cameron, *J. Am. Chem. Soc.*, 2013, **135**, 9362–9365.
15 R. Sunasee, C. K. Adokoh, J. Darkwa and R. Narain, *Expert Opin. Drug Deliv.*, 2014, **11**, 867–884.
16 N. Gaidzik, U. Westerlind and H. Kunz, *Chem. Soc. Rev.*, 2013, **42**, 4421–4442.
17 A. L. Martin, B. Li and E. R. Gillies, *J. Am. Chem. Soc.*, 2009, **131**, 734–741.
18 B.-S. Kim, D.-J. Hong, J. Bae and M. Lee, *J. Am. Chem. Soc.*, 2005, **127**, 16333–16337.
19 C. Schatz, S. Louguet, J.-F. Le Meins and S. Lecommandoux, *Angew. Chem. Int. Ed.*, 2009, **48**, 2572–2575.
20 C. Bonduelle, J. Huang, E. Ibarboure, A. Heise and S. Lecommandoux, *Chem. Commun.*, 2012, **48**, 8353.
21 S. Egli, H. Schlaad, N. Bruns and W. Meier, *Polymers*, 2011, **3**, 252–280.
22 G. Whitton and E. R. Gillies, *J. Polym. Sci. Part A: Polym. Chem.*, 2015, **53**, 148–172.
23 E. Blasco, M. Piñol and L. Oriol, *Macromol. Rapid Commun.*, 2014, **35**, 1090–1115.
24 E. R. Gillies, E. Dy, J. M. J. Fréchet and F. C. Szoka, *Mol. Pharm.*, 2005, **2**, 129–138.
25 C. C. Lee, E. R. Gillies, M. E. Fox, S. J. Guillaudeu, J. M. J. Fréchet, E. E. Dy and F. C. Szoka, *Proc. Natl. Acad. Sci.*, 2006, **103**, 16649–16654.
26 C. C. Lee, J. A. MacKay, J. M. J. Fréchet and F. C. Szoka, *Nat. Biotechnol.*, 2005, **23**, 1517–1526.
27 H. Ihre, O. L. Padilla De Jesús and J. M. J. Fréchet, *J. Am. Chem. Soc.*, 2001, **123**, 5908–5917.
28 M. Malkoch, E. Malmström and A. Hult, *Macromolecules*, 2002, **35**, 8307–8314.
29 B. Li, A. L. Martin and E. R. Gillies, *Chem. Commun.*, 2007, 5217.
30 S. J. van Vliet, E. Saeland and Y. van Kooyk, *Trends Immunol.*, 2008, **29**, 83–90.

31 U. Galili, *Immunol. Cell Biol.*, 2005, **83**, 674–686.
32 J. R. Kramer, A. R. Rodriguez, U.-J. Choe, D. T. Kamei and T. J. Deming, *Soft Matter*, 2013, **9**, 3389–3395.
33 D. Koester, A. Holkenbrink and D. Werz, *Synthesis*, 2010, **2010**, 3217–3242.
34 E. J. Cocinero, E. C. Stanca-Kaposta, M. Dethlefsen, B. Liu, D. P. Gamblin, B. G. Davis and J. P. Simons, *Chem. – Eur. J.*, 2009, **15**, 13427–13434.
35 R. A. Jockusch, R. T. Kroemer, F. O. Talbot, L. C. Snoek, P. Çarçabal, J. P. Simons, M. Havenith, J. M. Bakker, I. Compagnon, G. Meijer and G. von Helden, *J. Am. Chem. Soc.*, 2004, **126**, 5709–5714.
36 G. Yang, J. Schmieg, M. Tsuji and R. W. Franck, *Angew. Chem. Int. Ed.*, 2004, **43**, 3818–3822.
37 S. Liu and R. N. Ben, *Org. Lett.*, 2005, **7**, 2385–2388.
38 F. Nicotra, in *Glycoscience Synthesis of Substrate Analogs and Mimetics*, eds. D. H. Driguez and P. D. J. Thiem, Springer Berlin Heidelberg, 1997, pp. 55–83.
39 A. Nazemi, S. M. M. Haeryfar and E. R. Gillies, *Langmuir*, 2013, **29**, 6420–6428.
40 C. J. Capicciotti, J. F. Trant, M. Leclère and R. N. Ben, *Bioconjugate Chem.*, 2011, **22**, 605–616.
41 A. Nazemi, R. C. Amos, C. V. Bonduelle and E. R. Gillies, *J. Polym. Sci. Part A: Polym. Chem.*, 2011, **49**, 2546–2559.
42 H. Altin, I. Kosif and R. Sanyal, *Macromolecules*, 2010, **43**, 3801–3808.
43 P. Wu, M. Malkoch, J. N. Hunt, R. Vestberg, E. Kaltgrad, M. G. Finn, V. V. Fokin, K. B. Sharpless and C. J. Hawker, *Chem. Commun.*, 2005, 5775–5777.
44 W. Agut, R. Agnaou, S. Lecommandoux and D. Taton, *Macromol. Rapid Commun.*, 2008, **29**, 1147–1155.
45 G. J. M. Habraken, M. Peeters, C. H. J. T. Dietz, C. E. Koning and A. Heise, *Polym. Chem.*, 2010, **1**, 514–524.
46 D. Huesmann, A. Birke, K. Klinker, S. Türk, H. J. Räder and M. Barz, *Macromolecules*, 2014, **47**, 928–936.
47 S. Beychock, in *Poly-α-Amino Acids: Protein Models for Conformational Studies*, ed. G. D. Fasman, Marcel Dekker, Inc., New York, 1967, p. 293.
48 K. K. Upadhyay, J.-F. L. Meins, A. Misra, P. Voisin, V. Bouchaud, E. Ibarboure, C. Schatz and S. Lecommandoux, *Biomacromolecules*, 2009, **10**, 2802–2808.
49 B. K. Johnson and R. K. Prud'homme, *Phys. Rev. Lett.*, 2003, **91**, 118302-118305.
50 C. Sanson, C. Schatz, J.-F. Le Meins, A. Brûlet, A. Soum and S. Lecommandoux, *Langmuir*, 2010, **26**, 2751–2760.
51 M. Gkikas, J. S. Haataja, J. Seitsonen, J. Ruokolainen, O. Ikkala, H. Iatrou and N. Houbenov, *Biomacromolecules*, 2014, **15**, 3923–3930.
52. P. Heller, N. Mohr, A Birke, B. Weber, A. Reske-Kunz, M. Bros, M. Barz, *Macromol. Biosci.*, 2015, **15**, 63-73.
53 J.-W. Nah, Y.-I. Jeong, C.-S. Cho, S.-I. Kim, *J. Appl. Polym. Sci.* 2000, **75**, 1115-1126.
54 S. Lecommandoux, H.-A. Klok, M. Sayar and S. I. Stupp, *J. Polym. Sci. Part A: Polym. Chem.*, 2003, **41**, 3501–3518.
55 C. Bonduelle, S. Mazzaferro, J. Huang, O. Lambert, A. Heise and S. Lecommandoux, *Faraday Discuss.*, 2013, **166**, 137-150.
56 B. D. Olsen and R. A. Segalman, *Mater. Sci. Eng. Rep.*, 2008, **62**, 37–66.
57 P. G. de Gennes and H. Hervet, *J. Phys. Lett.*, 1983, **44**, 351–360.
58 K. Wang, G. Karlsson and M. Almgren, *J. Phys. Chem. B*, 1999, **103**, 9237–9246.
59 J. Jakeš, *Collect. Czechoslov. Chem. Commun.*, 1995, **60**, 1781–1797.

Table of contents entry

Polyester dendrons with peripheral α-galactose moieties were synthesized and coupled to poly(ɣ-benzyl-L-glutamate) to afford amphiphilic linear-dendron hybrid glycopolypeptides. These amphiphiles self-assembled in water to form micelles and other aggregates.